Mixture of Experts Enable Efficient and Effective Protein Understanding and Design

Ning Sun[1,2*], **Shuxian Zou**[1,2*], **Tianhua Tao**[1,4*], **Sazan Mahbub**[1,3*], **Dian Li**[1], **Yonghao Zhuang**[1,3*], **Hongyi Wang**[1], **Xingyi Cheng**[1,2], **Le Song**[1,2†], **Eric P. Xing**[1,2,3†]

[1]GenBio AI

[2]Mohamed bin Zayed University of Artificial Intelligence
[3]Carnegie Mellon University
[4]University of Washington

Abstract

Proteins play a fundamental role in life. Understanding the language of proteins offers significant potential for gaining mechanistic insights into biological systems and introduces new avenues for treating diseases, enhancing agriculture, and safeguarding the environment. While large protein language models (PLMs) like ESM2-15B and xTrimoPGLM-100B have achieved remarkable performance in diverse protein understanding and design tasks, these models, being dense transformer models, pose challenges due to their computational inefficiency during training and deployment. In this work, we introduce AIDO.Protein, a pretrained module for protein representation in an AI-driven Digital Organism [1]. AIDO.Protein is also the first mixture-of-experts (MoE) model in the protein domain, with model size scales to 16 billion parameters. Leveraging a sparse MoE architecture with 8 experts within each transformer block and selectively activating 2 experts for each input token, our model is significantly more efficient in training and inference. Through pre-training on 1.2 trillion amino acids collected from UniRef90 and ColabfoldDB, our model achieves state-of-the-art results across most tasks in the xTrimoPGLM benchmark. Furthermore, on over 280 ProteinGym Deep Mutational Scanning (DMS) assays, our model achieves nearly 99% of the overall performance of the best MSA-based model and significantly outperforms the previously reported state-of-the-art models that do not utilize MSA. We also adapted this model for structure-conditioned protein sequence generation tasks and achieved new SOTA in this domain. These results indicate that AIDO.Protein can serve as a strong foundation model for protein understanding and design. Models and codes are available through ModelGenerator in `https://github.com/genbio-ai/AIDO` and on Hugging Face.

1 Introduction

As the end product of genes, proteins serve as the workhorses of life, carrying out most of the biological functions within the cell. They act as biological catalysts, provide structural support to cells and tissues, facilitate the transport of molecules across cell membranes and within cells, recognize and neutralize foreign substances like pathogens, transmit signals that regulate cellular

*Work done during internship at GenBio AI.
†Corresponding authors: le.song@genbio.ai, eric.xing@genbio.ai

AI for New Drug Modalities at NeurIPS 2024.

processes, etc. To understand the function of a protein, a line of work follows the sequence-structure-function relationship, studying the structure first in order to understand its function since 3D structure is the active form of a protein [2]. Since protein structures are quite scarce, another line of work goes directly from sequence to function, aiming to determine the function given sequence-only information [3, 4]. Under both directions, we can see a common need to understand the language of protein sequences. Understanding the language of proteins is crucial to advancing genetic research and accelerating drug discovery. For example, it can help design enzymes that metabolize plastic waste or hydrolyse polluting toxins. It can also help create vaccines in a timely fashion during a pandemic.

Recent advances in artificial intelligence, especially the large language modeling technologies, offer promising avenues toward this goal. The huge success of large language models (LLMs) in natural language processing (NLP) inspire researchers to apply self-supervised pre-training in the protein domain, using protein sequences without any structural and functional labels [5, 6, 7, 8, 9, 10, 11, 12, 13, 3, 14, 15, 4]. These protein language models have demonstrated remarkable performance in a diverse array of tasks, including protein structure prediction, protein function prediction, and protein sequence design. For example, ESMFold based on protein language models [3] achieves atomic accuracy in protein structure prediction, reaching near AlphaFold2 [2] performance. xTrimoPGLM [4], a PLM at the scale of 100B parameters, obtains superior performance in diverse taks of protein function prediction. One of the key drive of performance is the scale of the PLM and we can see a clear trend that larger models have better performance. However, the computation efficiency will decrease when PLMs grow larger since running larger models is computationally more expensive. Exisiting work focus on pushing the performance of PLMs by scaling up model size without concerning much on the computation efficiency. Here we ask: *can we maintain/push the performance of a PLM while keeping it efficient during training and inference?*

We resort to sparse expert models for a potential solution. Sparse expert models are neural networks in which a subset of parameters is divided into "experts", each having a distinct weight. The models route input examples to specific expert(s) weights during training and inference. As a result, each example only interacts with a subset of the network parameters, different from dense models. Because only a fraction of the experts are used for each example, the amount of computation may remain small relative to the total model size [16]. Significant work has been done to investigate sparse expert models, of which, Mixture-of-Experts (MoE) stands out. Integrated into Transformer, MoE has become a strong counterpart of dense transformer models in the NLP domain [17, 18, 19].

In this work, we explore pre-training the first MoE model in the protein domain, different from all existing PLMs which adopt dense transformer architecture. We present AIDO.Protein, a MoE model at the scale of 16 billion parameters, pre-trained on 1.2 trillion tokens collected from UniRef90 and ColabfoldDB. During training and inference, each input token is processed by 4.5 billion parameters, using only 28% of the total number of parameters. We evaluate our model in a wide range of tasks, including 18 diverse tasks from xTrimoPGLM benchmark and 283 protein fitness prediction tasks from ProteinGym DMS benchmark. Experiment results show that AIDO.Protein achieves strong performance across the board while being more computational efficient. We further leverage AIDO.Protein for protein inverse folding and find that it outperforms previous SOTA methods, such as ProteinMPNN [20] and LM-Design [21]. These results demonstrate the effectiveness of AIDO.Protein in protein sequence understanding and design, providing the community with a new powerful and efficient protein foundation model.

2 Related work

2.1 Protein language model

Inspired by the huge success of large language models (LLMs) in the natural language processing (NLP) domain, in recent years, there has been a line of work applying LLM technologies in the protein domain [5, 6, 7, 8, 9, 10, 11, 12, 13, 3, 14, 15, 4].By pre-training on protein sequence databases, these protein language models have gain remarkable abilities in extracting biological meaningful representations for various downstream tasks, including protein structure and function predictions. In particular, ESM2 series, which scales up to 15 billion parameters, achieves atomic accuracy in protein structure prediction, demonstrating the effectiveness of large protein language model [3]. Recently, Chen et al. (2024) [4] pre-train a protein language model named xTrimoPGLM that conatains 100 billion parameters. It achieves superior performance on diverse tasks over ESM2-15B model, further

showcasing the effectiveness of scaling in the protein domain. However, these large protein language models are all dense transformer models, making finetuning for downstream tasks computational intensive especially for ESM2-15B and xTrimoPGLM-100B. In addition, the current largest open-source protein language model before our model is ESM2-15B since xTrimoPGLM-100B is not publicly available.

2.2 Mixture of experts

The scale of a model is one of the most important factors for better model quality. Given a fixed computing budget, training a larger model for fewer steps is better than training a smaller model for more steps [22]. Mixture of Experts (MoE) enable models to be pre-trained with far less compute, which means the model or dataset size can be dramatically scale up with the same compute budget as a dense model. It is a sparse neural network which leverages multiple expert networks, with a gating mechanism to select the most relevant experts for each input [23, 24]. This approach has gained prominence in large language models, where MoE layers replace dense MLP layers in transformers, allowing models to scale more efficiently by activating only a subset of experts for each token [16]. Key advancements include the GShard [17] and Switch Transformer [18], which improved training stability and efficiency through selective expert activation and load balancing strategies. The MoE design has also been successfully applied in vision transformers, with models like V-MoE [25] achieving comparable performance to dense models with significantly reduced computational costs. These developments highlight MoE's potential in both natural language processing and computer vision, offering scalable solutions for complex tasks. Recently, a powerful MoE model called Mixtral 8x7B [19] outperforms Llama 2 70B [26] and GPT-3.5 on most benchmarks while being more computational efficient during both training and inference. Inspired by its strong performance, we follow its architectural design in the MoE layers and pre-train a MoE model in the protein domain.

3 Pre-training AIDO.Protein

To scale up model size while maintaining a high training and inference efficiency, we opt for sparse MoE architecture and pre-train a powerful protein language model with 16 billion parameters on a carefully curated protein sequence database.

3.1 Model architecture

As shown in Figure 1, our model is a transformer encoder-only architecture with the dense MLP layer in each transformer block replaced by a sparse MoE layer. The MoE layer design largely follows Mixtral 8x7B [19]. The MoE layer is applied independently for each token in the input sequence. To be specific, suppose we have N experts $\{E_i(x), i = 1, ...N-1\}$, the output of the MoE layer y for each input token x is the weighted sum of the outputs of the expert networks, as shown in the following equation:

$$\begin{aligned} y &= \sum_{i=0}^{N-1} \text{Softmax}(\text{TopK}(x \cdot W_g)) \cdot E_i(x) \\ &= \sum_{i=0}^{N-1} \text{Softmax}(\text{TopK}(x \cdot W_g)) \cdot \text{SwiGLU}_i(x) \end{aligned} \tag{1}$$

where $W_g \in \mathcal{R}^{(d,N)}$ denotes the weight of the routing network (d is the hidden size), $E_i(x) = \text{SwiGLU}_i(x)$ denotes the i-th expert netwok. In our experiment, we set $N = 8, K = 2, d = 2304$. Our model contains 36 transformer layers and 36 attention heads, totaling 16 billion parameters. During training and inference, each input token is processed by 4.5 billion parameters, using only 28% of the total number of parameters.

AIDO.Protein is trained using the standard masked language modeling (MLM) objective. During training, the model predicts masked amino acids in a sequence, allowing it to learn the complex dependencies and relationships inherent in protein sequences. The use of MoE layers allows the model to allocate different experts to different types of sequence patterns, thus capturing a broader range of sequence features and enhancing its ability to predict and understand protein functions.

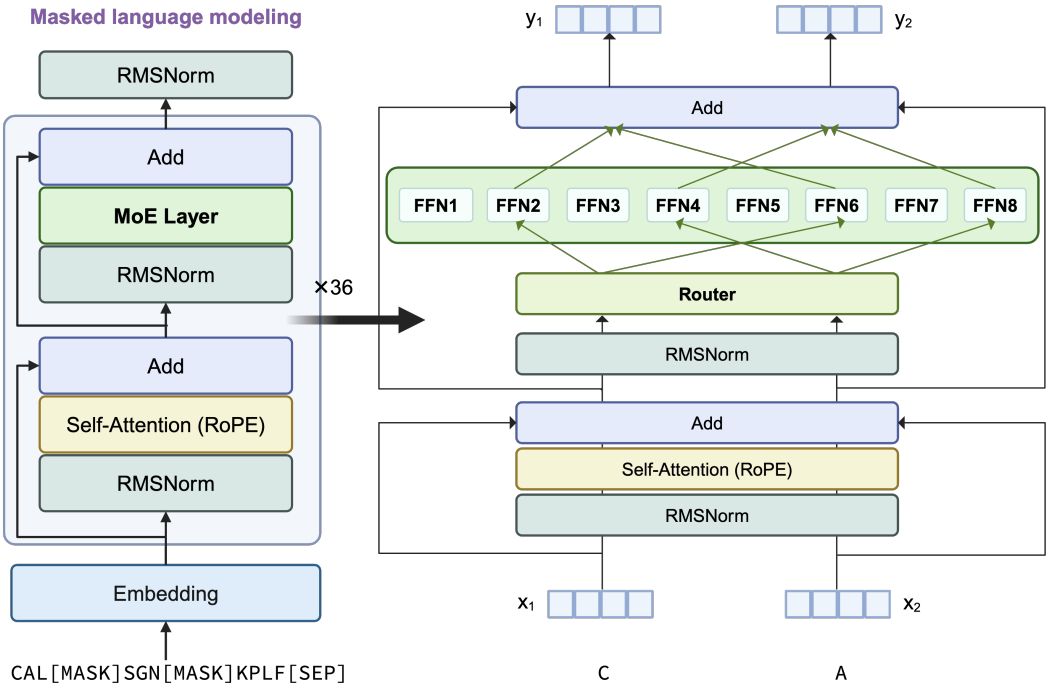

Figure 1: Model architecture of AIDO.Protein. We use sparse MoE architecture, with 8 experts in the Feed-Forward layer of a transformer block. For each token, 2 experts will be selectively activated by the top-2 routing mechanism. Figure created in BioRender.com.

3.2 Pre-training data

Inspired by previous work [27], We initially pre-trained our model on the combination of ColabfoldDB [28] and UniRef90 [29] databases. The ColabfoldDB emphasizes metagenomic data sources such as BFD [30], MGnify [31], and various eukaryotic and viral datasets, including SMAG [32], MetaEuk [33], TOPAZ [34], MGV [35], and GPD [36]. UniRef90 offers clustered sets of sequences from the UniProt Knowledgebase [3] and selected UniParc [4] records to achieve comprehensive coverage of the sequence space at multiple resolutions while minimizing data redundancy. Specifically, we utilize UniRef90/50 (before December 2022), which includes incremental data beyond the UniRef50/S representatives.

Given the effectiveness of UniRef90 for previous protein language models [37, 38, 3], and the observed benefits of continuous training on domain-specific data for enhancing downstream task performance[39], we further train on UniRef90 with an additional 100 billion tokens.

In summary, we developed two versions of AIDO.Protein: AIDO.Protein-16B trained on 1.2 trillion amino acids from ColabfoldDB and Uniref90, and AIDO.Protein-16B-v1 continuously trained on an additional 100 billion amino acids from Uniref90.

3.3 Pre-training settings

We use a global batch size of 2048 and context length of 2048. For optimizer, we use AdamW with weight decay of 0.1. The cosine learning rate schedule is employed with warmup ratio set to 2.5% of the total training steps. To accelerate training, we use FP16 mix precision training. We adopt Megatron-Deepspeed framework and pre-train our model using 256 Nvidia A100-80G GPUs for 25 days.

The pre-training process consists of three stages. In the first stage, the model was trained on 1 trillion tokens sampled from the UniRef90 and Colab databases over 18.5 days, with a learning rate starting

[3] `https://www.uniprot.org/help/uniprotkb`
[4] `https://www.uniprot.org/help/uniparc`

at 2e-4 and decaying to 2e-6. The second stage involved training on 200 billion tokens from the same data sources for 4 days, with the learning rate decreasing from 1e-5 to 1e-6. In the final stage, the model was further trained on 100 billion tokens from UniRef90, with a learning rate ranging between 1e-5 and 1e-6 for 2.5 days.

4 Experiments

We evaluate AIDO.Protein across more than 300 tasks from two important protein benchmarks, i.e., xTrimoPGLM benchmark [4] and ProteinGym DMS benchmark [40], encompassing residue-level, sequence-level, and protein-protein interaction (PPI) level tasks.

4.1 AIDO.Protein achieves strong results across diverse tasks from xTrimoPGLM benchmark

Tasks To fully test our model's ability in various protein understanding tasks, we evaluate our model on xTrimoPGLM benchmark [4]. It contains 18 diverse tasks which can be classified into four categories as follows:

- Protein structure prediction: **(1) Contact map prediction** aims to predict whether two residues i and j in a protein sequence are in contact or not based on their distance in the 3D structure with a threshold of 8Å. **(2) Fold prediction** aims to classify the protein sequence into one of the 1,195 known folds. **(3) Secondary structure prediction** aims to classify each residue into one of the 3 secondary structures, including Helix, Strand, and Coil.
- Protein function prediction: **(4) Antibiotic resistance prediction** aims to classify a protein sequence into one of the 19 antibiotics it is resistant to. **(5) Fluorescence prediction** aims to predict the fluorescence intensity of green fluorescent protein mutants. **(6) Fitness prediction** aims to to predict the fitness of GB1 binding following mutations. **(7) Localization prediction** aims to classify a protein sequence into one of the 10 subcellular localization categories.
- Protein-protein interaction prediction: **(8) Enzyme catalytic efficiency** aims to predict the enzymatic turnover numbers denoting the maximum chemical conversion rate of a reaction for a metabolic enzyme. **(9) Peptide-HLA/MHC affinity** aims to predict whether a given paired peptide and human leukocyte antigen (HLA) sequence can bind or not. **(10) Metal ion binding** aims to predict the existence of metal-ion binding site(s) on a given protein sequence. **(11) TCR pMHC affinity** aims to predict whether a given paired T cell receptor (TCR) sequence and peptide can bind or not.
- Protein development: **(12) Solubility** aims to predict whether a protein is soluble or insoluble. **(13) Stability** aims to predict the concentration of protease at which a protein can retain its folded state. **(14) Temperature stability** aims to predict a protein's capacity to preserve its structural stability under temperature 65 degree Celsius. **(15) Optimal temperature** aims to predict the optimal temperature for the catalytic activity of an enzyme. **(16) Optimal ph** aims to predict the optimal pH for the enzyme's reactions. **(17) Cloning clf** aims to predict whether a protein sequence tends to be a cloning failure or not. **(18) Material production** aims to predict whether a protein sequence fails at the protein material stage or not.

Fine-tuning models We use LoRA [41] for efficient finetuning on the 18 tasks. For sequence-level classification/regression tasks, for each input protein sequence [5], we perform mean pooling over the output hidden states of the transformer encoder and use a two-layer MLP network as the prediction head. For the contact map prediction, a token-level pairwise classification task, we first compute the outer product for the output hidden states of the transformer encoder to obtain a feature map, and then use a 2-layer MLP with inter hidden size 128 for prediction. For the secondary structure prediction, a token-level classification task, we use a two-layer MLP as the prediction head with the inter hidden size set to 128.

[5] For those tasks with multiple sequences as input, they are concatenated first using a `[SEP]` token before input to the model.

Table 1: AIDO.Protein-16B outperforms ESM2-15B on 14 out of 18 diverse tasks from the xTrimoPGLM benchmark. The results of ESM2-15B and xTrimoPGLM-100B are the LoRA finetuning results reported in [4]. Bold denotes the performance of our model is better than ESM2-15B.

Cate.	Task	Metric	AIDO.Protein-16B (ours)	ESM2-15B	xTrimoPGLM-100B
Protein Structure	contact prediction	Top L/5 ACC	**0.925**	0.922	0.933
	fold prediction	ACC	**0.763**	0.692	0.756
	secondary structure prediction	ACC	**0.874**	0.759	0.753
Protein Function	antibiotic resistance	ACC	0.979	0.983	0.984
	fluorescence prediction	Spearman CC	**0.679**	0.637	0.660
	fitness prediction	Spearman CC	**0.950**	0.948	0.961
	localization prediction	ACC	0.811	0.824	0.816
Protein Interaction	enzyme catalytic efficiency	Pearson CC	**0.749**	0.746	0.748
	metal ion binding	ACC	**0.824**	0.809	0.828
	peptide_HLA_MHC affinity	AUC	0.971	0.973	0.967
	tcr_pmhc affinity	AUC	**0.944**	0.941	0.951
Protein Development	solubility prediction	ACC	**0.806**	0.746	0.795
	stability prediction	Spearman CC	**0.824**	0.808	0.842
	temperature stability	MCC	0.932	0.932	0.942
	optimal temperature	Pearson CC	**0.798**	0.733	0.740
	optimal ph	Spearman CC	**0.640**	0.625	0.650
	cloning clf	AUC	**0.864**	0.766	0.848
	material production	AUC	**0.888**	0.792	0.865
	Average		**0.846**	0.813	0.835

Fine-tuning settings We follow the train/valid/test splits and evaluation metrics in the xTrimoPGLM benchmark [6]. For those tasks without validation sets, we randomly split 10% of training data for validation. For all tasks, we use LoRA fine-tuning with rank 16 and alpha 16. We use Adam optimizer with a peak learning rate 1e-4 and cosine learning rate scheduler with a warmup ratio of 0.05 for most of the tasks. For contact map prediction, we use Adam with a constant learning rate of 1e-4. We fine-tune the model for 10, 15 or 20 epochs and select the best checkpoints based on the validation scores. For details of hyperparameters for each tasks, please refer to our codebase.

Results Table 1 shows the results of our model on the xTrimoPGLM benchmark. On 14 out of 18 tasks, our model AIDO.Protein-16B achieves better results than ESM2-15B, demonstrating that our sparse MoE model is effective while being more efficient in both training and testing. On average across the 18 tasks, we achieve a average score of 0.846, outperforming both ESM2-15B and xTrimoPGLM-100B. In particular, our model excels in protein structure prediction and protein development tasks, indicating that it can serve a powerful foundation model for protein design.

4.2 AIDO.Protein demonstrates impressive performance on ProteinGym DMS benchmark

We further evaluate AIDO.Protein on ProteinGym DMS benchmark to fully test our model's ability in protein fitness prediction. This benchmark consists of 66 indels assays and 217 substitutions assays, with each assay providing all possible mutations for a specific target protein, along with their corresponding fitness scores. We adopt Spearman rank correlation and MSE as the evaluation metric. In the ProtienGym benchmarks, many methods are specialized and restricted to either indel or substitution tasks. We will focus mostly in comparing to methods which are versatile and generally applicable to both types of tasks. we will primarily compare our results with ESM-1v [37], Tranception [42], and MSA Transformer [43], with the latter two methods leveraging rich MSA information as input.

4.2.1 DMS indels supervised benchmark

Tasks Indel mutations are insertions or deletions of residues in a protein sequence. The DMS indels benchmark consists of 66 assays In machine learning, they can be formulated as sequence-level regression tasks. As shown in Table 2, the sample size for each task varies from 47 to 225,998, with $Q_3 = 193$. In particular, 54 tasks in the indels benchmark have sample sizes smaller or equal to 205. When evaluating under the 5-fold cross-validation setting, the small sample size makes an expressive

[6] `https://huggingface.co/Bo1015`

Table 2: Data statistics of ProteinGym DMS benchmark.

	Indels (66 assays)		**Substitutions (217 assays)**	
	target seq len	sample size	target seq len	sample size
mean	134	4,352	397	11,363
std	182	27,910	502	51,668
min	37	47	37	63
25%	52	121	69	1,332
50%	62	154	245	2,339
75%	72	193	536	6,769
max	770	225,998	3423	53,6962

Table 3: Results on ProteinGym DMS supervised benchmark. Bold denotes the best results, and underline denotes the second best results. AIDO.Protein achieves nearly 99% of the Spearman performance and superior MSE performance compared to Tranception Embeddings, the top MSA-based model in the overall DMS supervised benchmark, while significantly outperforming the previous state-of-the-art single-sequence model, ESM-1v.

Task Type	Model	Spearman by Functions					Avg. Spearman ↑	Avg. MSE ↓
		Activity	Expression	Fitness	Stability	Binding		
Indels 66 tasks	ESM-1v Embeddings	**0.706**	0.729	0.718	**0.856**	/	**0.752**	**0.365**
	Tranception Embeddings	0.674	**0.753**	0.716	0.797	/	0.735	0.410
	MSA Transformer Embeddings	0.661	0.614	0.710	0.769	/	0.689	0.486
	AIDO.Protein (ours)	0.698	0.721	**0.742**	0.829	/	0.748	0.370
Substutions 217 tasks	ESM-1v Embeddings	0.559	0.641	0.534	0.634	**0.881**	0.639	0.563
	Tranception Embeddings	**0.615**	**0.716**	**0.610**	0.872	0.672	**0.696**	**0.503**
	MSA Transformer Embeddings	0.596	0.632	0.523	0.886	0.564	0.642	0.573
	AIDO.Protein (ours)	0.574	0.677	0.569	**0.913**	0.675	0.682	0.509
Overall 283 tasks	ESM-1v Embeddings	0.593	0.662	0.577	0.686	**0.881**	0.665	0.517
	Tranception Embeddings	**0.629**	**0.725**	**0.635**	0.855	0.672	**0.705**	0.481
	MSA Transformer Embeddings	0.611	0.628	0.567	0.859	0.564	0.653	0.553
	AIDO.Protein (ours)	0.603	0.687	0.609	**0.893**	0.675	0.697	**0.477**

model prone to overfitting. Besides, the Spearnman rank correlation computed in a small validation set is not reliable for model selection. Therefore, we design different fine-tuning models for different tasks based on their sample sizes.

Fine-tuning settings Following the evaluation setting in ProteinGym, all the tasks are evaluated under a 5-fold cross-validation setting with the fold split in line with the *Random* cross-validation scheme provided by ProteinGym. For the 54 small tasks, we use linear probing with AIDO.Protein frozen to alleviate overfitting. The prediction head is a 2-layer MLP with the inter hidden size set to 128 and dropout rate set to 0.1. We use AdamW optimizer with a peak learning rate of 1e-3 and cosine learning scheduler with warmup ratio of 0.05. We do not use a validation set for model selection. Instead, we directly train the model to 1,000 steps and then use the last checkpoint to predict the test labels. For the other 12 tasks which contain more samples, we use LoRA fine-tuning with rank 16, alpha 32, and peak learning rate 1e-4. We use one fold for validation and train the model to 10,000 steps with early stopping. For all the tasks, the batch size B is determined by the sample size N using following rules: if $N \leq 100$, then $B = 4$; if $100 < N \leq 1000$, then $B = 8$; if $1000 < N \leq 5000$, then $B = 16$; if $5000 < N \leq 10000$, then $B = 32$; if $N > 10000$, then $B = 64$.

Results As shown in the upper section of Table 3, our model achieves 0.748 corrected average Spearman correlation across 66 indels assays, ranking in the second place across all models in the leaderboard [7]. Notably, the results of our model in terms of both mean square error (MSE) and Spearman correlation are very close to the SOTA model ESM-1v Embeddings [37]. And it achieves SOTA results in Fitness prediction, outperforming other models by large margins. Interestingly, our model outperforms MSA Transformer Embedding [43] and Tranception Embeddings [42], models that leverage homologous sequences for inference. This result indicates that protein language model

[7] `https://proteingym.org/benchmarks`

is better at handling sequences with insertion and deletions while MSA models are not robust enough in this case. Detailed performance for each indel task is available in the Appendix Figure 4.

4.2.2 DMS substitutions supervised benchmark

Tasks Substitution mutations involve replacing one or more residues in a protein sequence with different ones. The substitution benchmark includes 217 assays, comprising 69 single substitution assays and 148 multiple substitution assays. As shown in Table 2, the sequence length ranges from 37 to 3423, with sample size varying from 63 to 536962. For tasks with small sample sizes, the model is prone to overfitting. Additionally, for tasks with excessively long sequences, fine-tuning the model leads to OOM issues. Therefore, we apply different finetuning strategies for different tasks based on the sample size and sequence length.

Finetuning settings The ablation study in Appendix 5 shows that continuous pretraining on Uniref90 has significantly improved zero-shot substitution prediction, demonstrating the advantage of continuous training for substitution prediction. Therefore, we focus on evaluating AIDO.Protein-16B-v1, the version of AIDO.Protein-16B continuously trained on 100 billion amino acids from Uniref90, on the supervised substitution benchmark. ProteinGym provides three cross-validation schemes for the substitutions benchmark. To complete all tasks within reasonable time and resource constraints, we opted for the *Random* five-fold cross-validation scheme, consistent with the scheme used in the indels benchmark. We utilize the Adam optimizer and a cosine learning rate schedule. We employ LoRA [41] fine-tuning with a rank of 16 and alpha of 32, setting the peak learning rate to 1e-4 and training for 10,000 steps. Early stopping is triggered when the Spearman score on the validation set does not improve for predefined patience threshold. For 13 tasks with sample sizes exceeding 20,000, only one epoch per fold is performed, as a single pass through the data is sufficient. For 4 tasks with sequence lengths over 2048, we truncate the sequences to 2048 and adjust LoRA rank to 4 and alpha to 8. The batch size B and the early stopping patience P are determined by the sample size N using following rules: if $N \leq 100$, then $B = 4, P = 10$; if $100 < N \leq 1000$, then $B = 8, P = 5$; if $1000 < N \leq 5000$, then $B = 16, P = 3$; if $5000 < N \leq 10000$, then $B = 32, P = 3$; if $N > 10000$, then $B = 64, P = 1$.

Results As shown in middle section of Tab 3, our model achieves an average Spearman correlation of 0.682 and an mean square error (MSE) of 0.509 in supervised substitution benchmark, significantly outperforming previously reported best single-sequence based method, ESM-1v Embeddings, at both the functional group level and in average scores. Despite not utilizing MSA information, our model outperforms most MSA-based methods, such as the MSA Transformer, showcasing its strong ability to capture protein sequence information at the residue level. Furthermore, when compared to Tranception Embeddings, the leading MSA-based model in the overall DMS supervised benchmark, our model achieves comparable performance in both Spearman correlation and MSE metrics, and even surpasses Tranception Embeddings in the Stability and Binding functional groups. Further details on performance for each substitution task are provided in the Appendix Figure 3. Based on these comparisons, a promising direction for our future work would be to incorporate MSA into AIDO.Protein model for further improvements.

4.3 DMS overall supervised benchmark

Results In the bottom section of Tab 3, we finally evaluate our model's overall performance across 66 indels and 217 substitutions tasks. Even without leveraging MSA, our model achieves nearly 99% of the average Spearman correlation and superior MSE performance compared to the overall best MSA-based model, Tranception Embeddings, and significantly outperforms the previously reported state-of-the-art model, ESM-1v Embeddings, which also does not use MSA.

4.4 AIDO.Protein offers enhanced capabilities for protein design

Protein design is a vital area of research and application in biochemistry, molecular biology, and biotechnology [50, 12]. This section discusses the adaptation of AIDO.Protein for this purpose. Specifically, we develop a discrete diffusion modeling [51, 52] framework for protein inverse folding, a crucial step in *de novo* protein design, as discussed by Mu *et al.*[53]. We adopt ProteinMPNN-

Table 4: **Comparison of protein inverse folding performance.** Our protein design framework, with AIDO.Protein as the backbone, surpasses the performances of existing fixed-backbone protein inverse folding methods. The recovery rates of previous methods are quoted from [44].

Model	Median Sequence Recovery
StructTrans [45]	35.82 %
GVP [46]	39.47 %
ProteinMPNN [20]	45.96 %
ProteinMPNN-CMLM [21]	48.62 %
LM-Design [21]	54.41 %
DPLM [44]	54.54 %
AIDO.Protein-IFdiff (ours)	**58.26** %

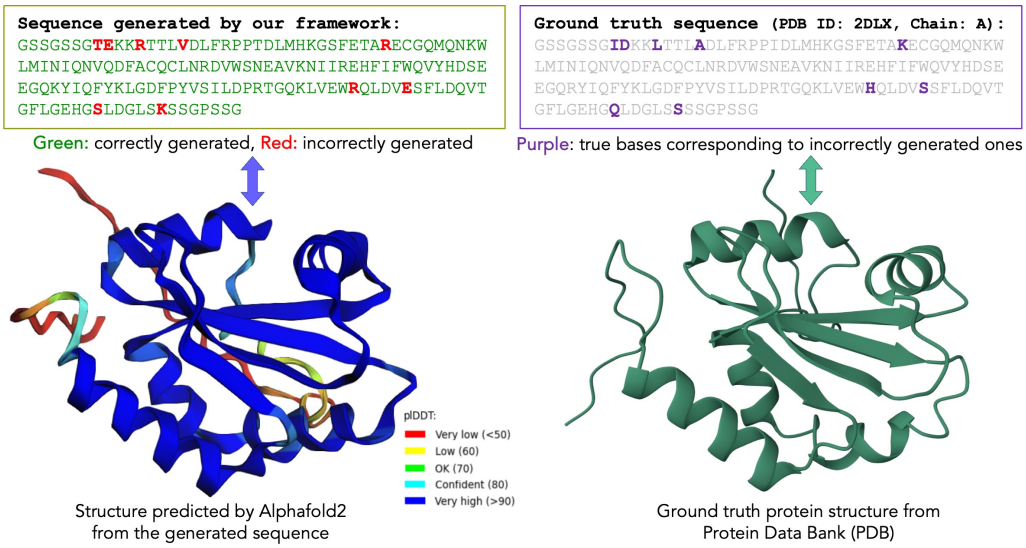

Figure 2: **An example result of our protein inverse folding framework** (PDB ID: 2DLX, Chain: A). **Left:** Our discrete diffusion based inverse folding framework generates the protein sequence. We then use AlphaFold2 [47] to predict its structure from the generated sequence for analysis. The confidence of structure prediction, measured with pIDDT [47], is shown with color-codes. We use ColabFold [48] framework for AlphaFold2-based inference and rendering the protein molecule. **Right:** Ground truth protein sequence and structure from Protein Data Bank [49].

CMLM, a variant of ProteinMPNN [20] produced by [21], as our structure encoder for structure-conditioned diffusion. Details about the framework are available in Appendix A.1.

For experiments, we use the dataset by CATH 4.2 dataset [54], a well-established resource for evaluating protein design. In Table 4, we show our framework, denoted as AIDO.ProteinIF, achieves significantly higher score than the previous state-of-the-art methods.

In Figure 2, we show an example generated protein by our framework and the ground truth from PDB [49].

5 Conclusions and future work

In this paper, we introduce AIDO.Protein, a 16 billion parameter protein language model that incorporates mixture-of-expert layers and is trained on 1.2 trillion amino acids from ColabfoldDB and UniRef90. To our knowledge, our work is the first application of sparse expert models in the protein domain, allowing for efficient modeling while maintaining high performance. AIDO.Protein demonstrates exceptional performance across various protein understanding tasks, achieving state-of-the-art (SOTA) results on most xTrimoPGLM tasks and ranking second on the ProteinGym DMS

leaderboard. Additionally, it showcases remarkable potential in de novo protein design through inverse folding. This dual proficiency in understanding and generating proteins underscores the model's value in advancing drug discovery, personalized medicine, enzyme engineering, and immune response prediction. Its capabilities position AIDO.Protein as a catalyst for significant innovations in biotechnology and synthetic biology, paving the way for new solutions and applications in these critical fields.

References

[1] Le Song, Eran Segal, and Eric Xing. Toward AI-Driven Digital Organism: Multiscale Foundation Models for Predicting, Simulating, and Programming Biology at All Levels . *Technical Report*, 2024.

[2] Jumper John, Evans Richard, Pritzel Alexander, Green Tim, Figurnov Michael, Ronneberger Olaf, Tunyasuvunakool Kathryn, Bates Russ, Žídek Augustin, Potapenko Anna, et al. Highly accurate protein structure prediction with alphafold. *Nature*, 2021.

[3] Zeming Lin, Halil Akin, Roshan Rao, Brian Hie, Zhongkai Zhu, Wenting Lu, Nikita Smetanin, Robert Verkuil, Ori Kabeli, Yaniv Shmueli, Allan dos Santos Costa, Maryam Fazel-Zarandi, Tom Sercu, Salvatore Candido, and Alexander Rives. Evolutionary-scale prediction of atomic-level protein structure with a language model. *Science*, 379(6637):1123–1130, 2023.

[4] Bo Chen, Xingyi Cheng, Pan Li, Yangli-ao Geng, Jing Gong, Shen Li, Zhilei Bei, Xu Tan, Boyan Wang, Xin Zeng, et al. xtrimopglm: unified 100b-scale pre-trained transformer for deciphering the language of protein. *arXiv preprint arXiv:2401.06199*, 2024.

[5] Roshan Rao, Nicholas Bhattacharya, Neil Thomas, Yan Duan, Peter Chen, John Canny, Pieter Abbeel, and Yun Song. Evaluating protein transfer learning with tape. *Advances in neural information processing systems*, 32, 2019.

[6] Ethan C Alley, Grigory Khimulya, Surojit Biswas, Mohammed AlQuraishi, and George M Church. Unified rational protein engineering with sequence-based deep representation learning. *Nature methods*, 16(12):1315–1322, 2019.

[7] Alexander Rives, Joshua Meier, Tom Sercu, Siddharth Goyal, Zeming Lin, Jason Liu, Demi Guo, Myle Ott, C. Lawrence Zitnick, Jerry Ma, and Rob Fergus. Biological structure and function emerge from scaling unsupervised learning to 250 million protein sequences. *PNAS*, 2019.

[8] Ali Madani, Ben Krause, Eric R Greene, Subu Subramanian, Benjamin P Mohr, James M Holton, Jose Luis Olmos, Caiming Xiong, Zachary Z Sun, Richard Socher, et al. Large language models generate functional protein sequences across diverse families. *Nature Biotechnology*, 41(8):1099–1106, 2023.

[9] Ahmed Elnaggar, Michael Heinzinger, Christian Dallago, Ghalia Rihawi, Yu Wang, Llion Jones, Tom Gibbs, Tamas Feher, Christoph Angerer, Martin Steinegger, Debsindhu Bhowmik, and Burkhard Rost. Prottrans: Towards cracking the language of life's code through self-supervised deep learning and high performance computing, 2021.

[10] Jung-Eun Shin, Adam J Riesselman, Aaron W Kollasch, Conor McMahon, Elana Simon, Chris Sander, Aashish Manglik, Andrew C Kruse, and Debora S Marks. Protein design and variant prediction using autoregressive generative models. *Nature communications*, 12(1):2403, 2021.

[11] Joshua Meier, Roshan Rao, Robert Verkuil, Jason Liu, Tom Sercu, and Alex Rives. Language models enable zero-shot prediction of the effects of mutations on protein function. *Advances in neural information processing systems*, 34:29287–29303, 2021.

[12] Noelia Ferruz, Steffen Schmidt, and Birte Höcker. Protgpt2 is a deep unsupervised language model for protein design. *Nature communications*, 13(1):4348, 2022.

[13] Ratul Chowdhury, Nazim Bouatta, Surojit Biswas, Christina Floristean, Anant Kharkar, Koushik Roy, Charlotte Rochereau, Gustaf Ahdritz, Joanna Zhang, George M Church, et al. Single-sequence protein structure prediction using a language model and deep learning. *Nature Biotechnology*, 40(11):1617–1623, 2022.

[14] Ruidong Wu, Fan Ding, Rui Wang, Rui Shen, Xiwen Zhang, Shitong Luo, Chenpeng Su, Zuofan Wu, Qi Xie, Bonnie Berger, et al. High-resolution de novo structure prediction from primary sequence. *BioRxiv*, pages 2022–07, 2022.

[15] Xiaomin Fang, Fan Wang, Lihang Liu, Jingzhou He, Dayong Lin, Yingfei Xiang, Kunrui Zhu, Xiaonan Zhang, Hua Wu, Hui Li, et al. A method for multiple-sequence-alignment-free protein structure prediction using a protein language model. *Nature Machine Intelligence*, 5(10):1087–1096, 2023.

[16] William Fedus, Jeff Dean, and Barret Zoph. A review of sparse expert models in deep learning. *arXiv preprint arXiv:2209.01667*, 2022.

[17] Dmitry Lepikhin, HyoukJoong Lee, Yuanzhong Xu, Dehao Chen, Orhan Firat, Yanping Huang, Maxim Krikun, Noam Shazeer, and Zhifeng Chen. Gshard: Scaling giant models with conditional computation and automatic sharding. *arXiv preprint arXiv:2006.16668*, 2020.

[18] William Fedus, Barret Zoph, and Noam Shazeer. Switch transformers: Scaling to trillion parameter models with simple and efficient sparsity. *Journal of Machine Learning Research*, 23(120):1–39, 2022.

[19] Albert Q Jiang, Alexandre Sablayrolles, Antoine Roux, Arthur Mensch, Blanche Savary, Chris Bamford, Devendra Singh Chaplot, Diego de las Casas, Emma Bou Hanna, Florian Bressand, et al. Mixtral of experts. *arXiv preprint arXiv:2401.04088*, 2024.

[20] Justas Dauparas, Ivan Anishchenko, Nathaniel Bennett, Hua Bai, Robert J Ragotte, Lukas F Milles, Basile IM Wicky, Alexis Courbet, Rob J de Haas, Neville Bethel, et al. Robust deep learning–based protein sequence design using proteinmpnn. *Science*, 378(6615):49–56, 2022.

[21] Zaixiang Zheng, Yifan Deng, Dongyu Xue, Yi Zhou, Fei Ye, and Quanquan Gu. Structure-informed language models are protein designers. In *International conference on machine learning*, pages 42317–42338. PMLR, 2023.

[22] Jared Kaplan, Sam McCandlish, Tom Henighan, Tom B Brown, Benjamin Chess, Rewon Child, Scott Gray, Alec Radford, Jeffrey Wu, and Dario Amodei. Scaling laws for neural language models. *arXiv preprint arXiv:2001.08361*, 2020.

[23] Robert A Jacobs, Michael I Jordan, Steven J Nowlan, and Geoffrey E Hinton. Adaptive mixtures of local experts. *Neural computation*, 3(1):79–87, 1991.

[24] Noam Shazeer, Azalia Mirhoseini, Krzysztof Maziarz, Andy Davis, Quoc Le, Geoffrey Hinton, and Jeff Dean. Outrageously large neural networks: The sparsely-gated mixture-of-experts layer. *arXiv preprint arXiv:1701.06538*, 2017.

[25] Carlos Riquelme, Joan Puigcerver, Basil Mustafa, Maxim Neumann, Rodolphe Jenatton, André Susano Pinto, Daniel Keysers, and Neil Houlsby. Scaling vision with sparse mixture of experts. *Advances in Neural Information Processing Systems*, 34:8583–8595, 2021.

[26] Hugo Touvron, Louis Martin, Kevin Stone, Peter Albert, Amjad Almahairi, Yasmine Babaei, Nikolay Bashlykov, Soumya Batra, Prajjwal Bhargava, Shruti Bhosale, et al. Llama 2: Open foundation and fine-tuned chat models. *arXiv preprint arXiv:2307.09288*, 2023.

[27] Xingyi Cheng, Bo Chen, Pan Li, Jing Gong, Jie Tang, and Le Song. Training compute-optimal protein language models. *bioRxiv*, pages 2024–06, 2024.

[28] Mirdita Milot, Schütze Konstantin, Moriwaki Yoshitaka, Heo Lim, Ovchinnikov Sergey, and Steinegger Martin. Colabfold: making protein folding accessible to all. *Nature methods*, 2022.

[29] Suzek Baris, E, Wang Yuqi, Huang Hongzhan, McGarvey Peter, B, Wu Cathy, H, and UniProt Consortium. Uniref clusters: a comprehensive and scalable alternative for improving sequence similarity searches. *Bioinformatics, 31(6):926–932*, 2015.

[30] Bfd- big fantastic database.

[31] Mitchell Alex, L, Almeida Alexandre, Beracochea Martin, Boland Miguel, Burgin Josephine, Cochrane Guy, Crusoe Michael, R, Kale Varsha, Potter Simon, C, Richardson Lorna, J, et al. Mgnify: the microbiome analysis resource in 2020. *Nucleic acids research*, 2020.

[32] Delmont Tom, O, Gaia Morgan, Hinsinger Damien, D, Frémont Paul, Vanni Chiara, Fernandez-Guerra Antonio, Eren A, Murat, Kourlaiev Artem, d'Agata Leo, Clayssen Quentin, et al. Functional repertoire convergence of distantly related eukaryotic plankton lineages abundant in the sunlit ocean. *Cell Genomics*, 2022.

[33] Karin Eli, Levy, Mirdita Milot, and Söding Johannes. Metaeuk—sensitive, high-throughput gene discovery, and annotation for large-scale eukaryotic metagenomics. *Microbiome*, 2020.

[34] Alexander Harriet, Hu Sarah, K, Krinos Arianna, I, Pachiadaki Maria, Tully Benjamin, J, Neely Christopher, J, and Reiter Taylor. Eukaryotic genomes from a global metagenomic dataset illuminate trophic modes and biogeography of ocean plankton. *bioRxiv, pages 2021–07*, 2021.

[35] Nayfach Stephen, Páez-Espino David, Call Lee, Low Soo, Jen, Sberro Hila, Ivanova Natalia, N, Proal Amy, D, Fischbach Michael, A, Bhatt Ami, S, Hugenholtz Philip, et al. Metagenomic compendium of 189,680 dna viruses from the human gut microbiome. *Nature microbiology*, 2021.

[36] Camarillo-Guerrero Luis, F, Almeida Alexandre, Rangel-Pineros Guillermo, Finn Robert, D, and Lawley Trevor, D. Massive expansion of human gut bacteriophage diversity. *Cell*, 2021.

[37] Joshua Meier, Roshan Rao, Robert Verkuil, Jason Liu, Tom Sercu, and Alexander Rives. Language models enable zero-shot prediction of the effects of mutations on protein function. *bioRxiv*, 2021.

[38] Brandes Nadav, Goldman Grant, Wang Charlotte, H., Ye Chun, Jimmie, and Ntranos Vasilis. Genome-wide prediction of disease variant effects with a deep protein language model. *Nature Genetics*, 2023.

[39] Gururangan Suchin, Marasovic Ana, Swayamdipta Swabha, Lo Kyle, Beltagy Iz, Downey Doug, and Smith Noah, A. Don't stop pretraining: Adapt language models to domains and tasks. *ACL*, 2020.

[40] Pascal Notin, Aaron Kollasch, Daniel Ritter, Lood Van Niekerk, Steffanie Paul, Han Spinner, Nathan Rollins, Ada Shaw, Rose Orenbuch, Ruben Weitzman, et al. Proteingym: Large-scale benchmarks for protein fitness prediction and design. *Advances in Neural Information Processing Systems*, 36, 2024.

[41] Edward J Hu, Yelong Shen, Phillip Wallis, Zeyuan Allen-Zhu, Yuanzhi Li, Shean Wang, Lu Wang, and Weizhu Chen. Lora: Low-rank adaptation of large language models. *arXiv preprint arXiv:2106.09685*, 2021.

[42] Pascal Notin, Mafalda Dias, Jonathan Frazer, Javier Marchena-Hurtado, Aidan N Gomez, Debora Marks, and Yarin Gal. Tranception: protein fitness prediction with autoregressive transformers and inference-time retrieval. In *International Conference on Machine Learning*, pages 16990–17017. PMLR, 2022.

[43] Roshan Rao, Jason Liu, Robert Verkuil, Joshua Meier, John F. Canny, Pieter Abbeel, Tom Sercu, and Alexander Rives. Msa transformer. *bioRxiv*, 2021.

[44] Xinyou Wang, Zaixiang Zheng, Fei Ye, Dongyu Xue, Shujian Huang, and Quanquan Gu. Diffusion language models are versatile protein learners. *arXiv preprint arXiv:2402.18567*, 2024.

[45] John Ingraham, Vikas Garg, Regina Barzilay, and Tommi Jaakkola. Generative models for graph-based protein design. *Advances in neural information processing systems*, 32, 2019.

[46] Bowen Jing, Stephan Eismann, Patricia Suriana, Raphael John Lamarre Townshend, and Ron Dror. Learning from protein structure with geometric vector perceptrons. In *International Conference on Learning Representations*, 2020.

[47] John Jumper, Richard Evans, Alexander Pritzel, Tim Green, Michael Figurnov, Olaf Ronneberger, Kathryn Tunyasuvunakool, Russ Bates, Augustin Žídek, Anna Potapenko, et al. Highly accurate protein structure prediction with alphafold. *nature*, 596(7873):583–589, 2021.

[48] Milot Mirdita, Konstantin Schütze, Yoshitaka Moriwaki, Lim Heo, Sergey Ovchinnikov, and Martin Steinegger. Colabfold: making protein folding accessible to all. *Nature methods*, 19(6):679–682, 2022.

[49] Protein Data Bank. Protein data bank. *Nature New Biol*, 233(223):10–1038, 1971.

[50] Ivan V Korendovych and William F DeGrado. De novo protein design, a retrospective. *Quarterly reviews of biophysics*, 53:e3, 2020.

[51] Subham Sekhar Sahoo, Marianne Arriola, Yair Schiff, Aaron Gokaslan, Edgar Marroquin, Justin T Chiu, Alexander Rush, and Volodymyr Kuleshov. Simple and effective masked diffusion language models. *arXiv preprint arXiv:2406.07524*, 2024.

[52] Lin Zheng, Jianbo Yuan, Lei Yu, and Lingpeng Kong. A reparameterized discrete diffusion model for text generation. *arXiv preprint arXiv:2302.05737*, 2023.

[53] Junxi Mu, Zhengxin Li, Bo Zhang, Qi Zhang, Jamshed Iqbal, Abdul Wadood, Ting Wei, Yan Feng, and Hai-Feng Chen. Graphormer supervised de novo protein design method and function validation. *Briefings in Bioinformatics*, 25(3):bbae135, 2024.

[54] Christine A Orengo, Alex D Michie, Susan Jones, David T Jones, Mark B Swindells, and Janet M Thornton. Cath–a hierarchic classification of protein domain structures. *Structure*, 5(8):1093–1109, 1997.

[55] Jonathan Ho, Ajay Jain, and Pieter Abbeel. Denoising diffusion probabilistic models. *Advances in neural information processing systems*, 33:6840–6851, 2020.

[56] Jacob Austin, Daniel D Johnson, Jonathan Ho, Daniel Tarlow, and Rianne Van Den Berg. Structured denoising diffusion models in discrete state-spaces. *Advances in Neural Information Processing Systems*, 34:17981–17993, 2021.

[57] John R Hershey and Peder A Olsen. Approximating the kullback leibler divergence between gaussian mixture models. In *2007 IEEE International Conference on Acoustics, Speech and Signal Processing-ICASSP'07*, volume 4, pages IV–317. IEEE, 2007.

[58] Diederik Kingma, Tim Salimans, Ben Poole, and Jonathan Ho. Variational diffusion models. *Advances in neural information processing systems*, 34:21696–21707, 2021.

[59] A Vaswani. Attention is all you need. *Advances in Neural Information Processing Systems*, 2017.

[60] Neil Houlsby, Andrei Giurgiu, Stanislaw Jastrzebski, Bruna Morrone, Quentin De Laroussilhe, Andrea Gesmundo, Mona Attariyan, and Sylvain Gelly. Parameter-efficient transfer learning for nlp. In *International conference on machine learning*, pages 2790–2799. PMLR, 2019.

[61] Ke Zixuan, Shao Yijia, Lin Haowei, Konishi Tatsuya, Kim1 Gyuhak, and Liu Bing. Continual pre-training of language models. *arXiv:2302.03241*, 2023.

[62] Greco Claudio, Plank Barbara, Fernández Raquel, and Bernardi Raffaella. Psycholinguistics meets continual learning: Measuring catastrophic forgetting in visual question answering. *arXiv preprint arXiv:1906.04229*, 2019.

A Experiments

A.1 Protein Design

A.1.1 Masked Diffusion for Protein Sequence Generation

We aim to approximate a data distribution $q(x)$ by training a diffusion model, by first iteratively adding noise to a sample $x_0 \sim q(x)$ for T discrete steps (forward process) that results in a sample with entire noise x_T; and then training a model, parameterized by θ, to denoise x_T iteratively to retrieve the original signal x_0 (reverse process). In case of continuous signal, such as image or audio, at any time-step $t \in [0, T]$, the sample x_t can be assumed as a linear combination of the original signal x_0 and Gaussian noise $\epsilon \sim \mathcal{N}(0, 1)$ [55],

$$x_t = \sqrt{\pi(t)}\, x_0 + \sqrt{1 - \pi(t)}\, \epsilon, \tag{2}$$

where $\pi(.) \in [0, 1]$ is a monotonically decreasing function of time-step t. The model learns a marginal distribution $p_\theta(x_{t-1}|x_t)$, which aims to approximate the true transition probability $q(x_{t-1}|x_t, x_0)$ of estimating a less noisy variant x_{t-1} given a relatively more noisy variant x_t.

Given that, at $t = 0$ we have $x_t = x_0$ (with $\pi(t) = 1$), and at $t = T$, $x_t = x_T = \epsilon \sim \mathcal{N}(0, 1)$ (with $\pi(t) = 0$) that is pure Gaussian noise. However, in case of discrete signals like protein sequence, this is infeasible to represent x_T as a samples from unit-Gaussian. We can, instead, represent x_T entirely by *absorbing state* [51, 56] that contain no data-specific signal, i.e., analogous to pure Gaussian noise. Following [56], we use `[MASK]` token as the absorbing state.

For our masked diffusion model training objective, we adopt the formulation proposed by [51]. Overall the objective function for diffusion, negative evidence lower bound on log likelihood (NELBO) [56], can be decoupled into three disjoint objectives for reconstruction $\mathcal{J}_{recon}$, diffusion $\mathcal{J}_{diff}$, and prior $\mathcal{J}_{prior}$. As derived by [56, 51, 52], it is possible to show that for diffusion directly on data samples x, $\mathcal{J}_{recon},\ \mathcal{J}_{prior} = 0$. Given this, NELBO for discrete times-steps T simplifies to,

$$\mathcal{J}^{<T>} = \mathcal{J}_{diff} = -\mathbb{E}_{t\sim\mathcal{U}[1,T],\ x_0\sim q,\ x_{t-1}\sim p_\theta}\Big[\frac{\pi(t-1) - \pi(t)}{\pi(0) - \pi(t)} \log\langle x_{t-1}, x_0\rangle\Big], \tag{3}$$

where $\mathcal{U}[1, T]$ is a uniform distribution integers between 1 and T, and $\langle x_{t-1}, x_0\rangle$ computes the similarity between x_{t-1} and x_0. Equation 3 is derived from the Kullback–Leibler divergence [57] between the transition probability distributions q and p. Please find the detailed derivation in [51].

In this study, we adopt cross-entropy loss between x_0 and x_{t-1}, $\mathcal{L}_{CE}(x_0, x_{t-1})$, for $-\log\langle x_{t-1}, x_0\rangle$. [58] showed that, with higher number of diffusion steps T, we can get a tighter bound on $\mathcal{J}^{<T>}$. With $T \to \infty$, Equation 3 becomes,

$$\mathcal{J}^{<T\to\infty>} = \mathbb{E}_{t\sim\mathcal{U}[1,\infty),\ x_0\sim q,\ x_{t-1}\sim p_\theta}\Big[\frac{\pi(t-1) - \pi(t)}{1 - \pi(t)} \mathcal{L}_{CE}(x_0, x_{t-1})\Big], \tag{4}$$

where $\pi(0) = 1$. Please note that, for $T \to \infty$, $\pi(t-1) \to \pi(t)$, i.e., the change in $\pi(.)$ at any time t should be infinitesimally small. Also, since $\pi(.)$ is monotonically decreasing, $\pi(t-1) - \pi(t) > 0$. With $T \to \infty$, we can represent this change with the negative time-derivative of $\pi(.)$ at time t, $-\frac{d\pi(t)}{dt} = -\pi'(t)$. This leads to the continuous-time likelihood bound,

$$\mathcal{J}^{<T\to\infty>} = -\mathbb{E}_{t\sim\mathcal{U}[1,\infty),\ x_0\sim q,\ x_{t-1}\sim p_\theta}\Big[\frac{\pi'(t)}{1 - \pi(t)} \mathcal{L}_{CE}(x_0, x_{t-1})\Big]. \tag{5}$$

As shown by [51], the choice of $\pi(.)$ has insignificant effect on the overall performance of the training algorithm. We adopt $\pi(.) = 1 - \frac{t}{T}; \forall t \in [1, \infty)$ as our noise schedule. This further simplifies Equation 5 as,

$$\mathcal{J}^{<T\to\infty>} = \mathbb{E}_{t\sim\mathcal{U}[1,\infty),\ x_0\sim q,\ x_{t-1}\sim p_\theta}\Big[\frac{\mathcal{L}_{CE}(x_0, x_{t-1})}{t}\Big]. \tag{6}$$

Intuition behind the objective function. Note that the loss computed on any sample x_t is now inversely proportional to t. Intuitively, if t is large, x_t is more noisy and hence it can potentially lead to many varieties of reconstructed samples $\hat{x}$ from $q(x)$, i.e., all of them can be valid. However, with $\mathcal{L}_{CE}(x_0, x_t)$ loss we are always pushing the x_t to be more similar to x_0, i.e., encouraging less diversity in generation, which is only expected if x_t is already very similar to x_0 (when t is smaller). To address this conflict, the loss $\mathcal{L}_{CE}(x_0, x_t)$ is down-weighted by the factor $\frac{1}{t}$.

A.1.2 Protein Inverse Folding

Protein inverse folding represents a cutting-edge computational technique aimed at generating protein sequences that will fold into specific three-dimensional structures [21, 20]. This innovative approach stands in stark contrast to traditional methods of protein folding, where the primary goal is to predict the 3D structure based on an existing protein sequence [2].

The central challenge in protein inverse folding involves identifying sequences capable of reliably adopting the intended structure [21, 44]. In our research, we concentrate on designing sequences based on the known backbone structure of a protein [21, 20, 44]. This is particularly crucial for fields like synthetic biology and nanotechnology, where the development of specific protein structures is essential for executing vital biological functions [50]. Recent advances in computational modeling, particularly those leveraging deep generative models, have significantly improved the accessibility and effectiveness of protein inverse folding approaches [21, 44, 20].

In the following part, we discuss how we adapt our AIDO.Protein with masked diffusion modeling conditioned on 3D protein structures.

Adaptation with Conditional Diffusion. During training, we aim to optimize the diffusion objective described in Equation 6. We start by sampling a sequence x_0 with a known 3D protein structure and masking a fraction $\frac{t}{T}$ (where $t \sim \mathcal{U}[1, T]$). This results in x_t, which acts as a noisy variant of x_0. We then pass x_t through ProteinMPNN-CMLM [21], generating an initial estimate of the sequence S_t and a structural embedding e_t^{st}.

This S_t is subsequently processed by the encoder of AIDO.Protein, producing the sequence embedding e_t^{seq}. Following this, e_t^{st} and e_t^{seq} are input into an adaptor module [44, 21], which, in our design, consists of a multihead self-attention layer [59] combined with a bottleneck multi-layer perceptron [60], generating a new estimate of the protein sequence, x_{t-1}. Note that the framework described above models the transition function $p_\theta(x_{t-1}|x_t)$.

After the training is completed, we can generate sequences using our framework. We begin by providing the generation framework with a sequence composed solely of mask tokens, denoted by x_T, along with the protein structure. The output x_{T-1} is anticipated to be a less noisy version of the expected ground truth x_0. We then iteratively denoise this sequence over multiple steps to produce our final generated sequence $\hat{x}_0$.

A.2 AIDO.Protein Performance on DMS Substitution and Indel Benchmarks

A.3 Ablation Studies of Continuous Training

In this section, we further explore the impact of continuous training and how the choice of continuous training datasets affects downstream performance.

A.3.1 Influence of continuous training on model effectiveness

Previous studies [61, 39, 62] have shown that continuous training on domain-specific datasets can significantly improve performance on downstream tasks. We compare three models: the first is trained on 1 trillion tokens from UniMeta, the second continues with an additional 200 billion UniMeta tokens at a reduced learning rate, and the third focuses on UniRef90, a subset of UniMeta, with an additional 100 billion tokens. The performance of these three models on the DMS zero-shot benchmark is presented in Table 5. We observe that training on more UniMeta tokens significantly improves performance, and continuous training on a more domain-specific dataset, like UniRef90, further enhances results.

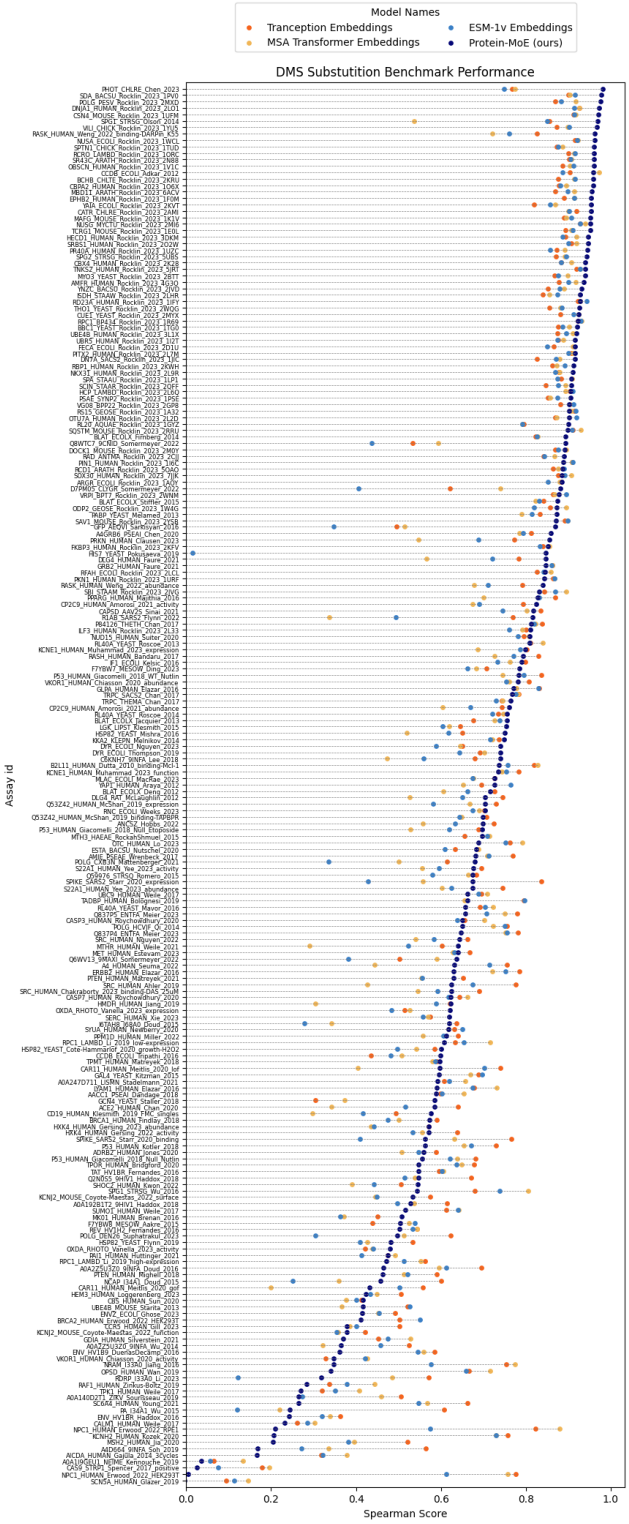

Figure 3: Spearman correlation performance on each assay from the substitution benchmark. We compared our AIDO.Protein (in dark blue) with the top 3 models in the overall DMS benchmark: Tranception (in orange) and MSA Transformer (in yellow), both of which are MSA-based, and ESM-1v (in light blue), which uses single sequence inputs. AIDO.Protein outperforms MSA Transformer and ESM-1v on most tasks, achieving performance close to Tranception.

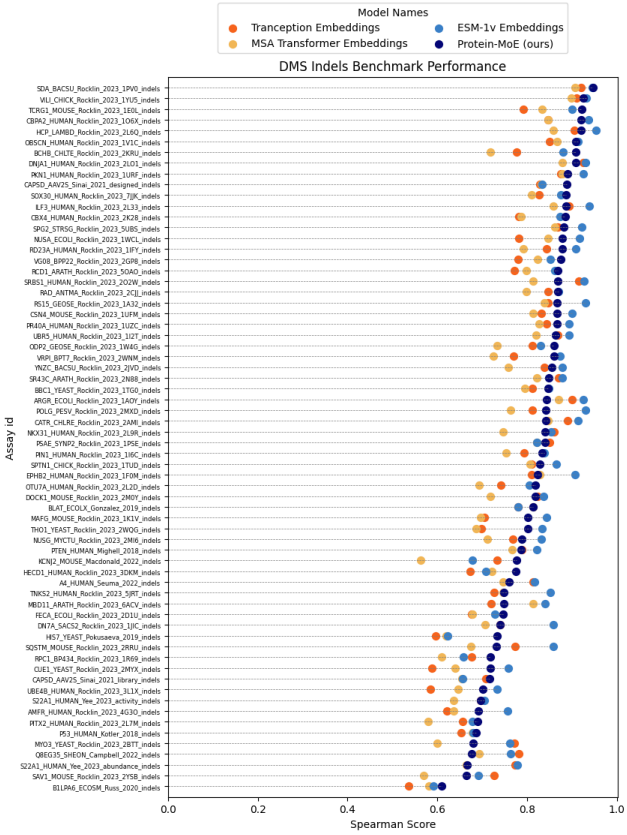

Figure 4: Spearman correlation performance on 66 indels assays from DMS indels benchmark. We compared our AIDO.Protein (in dark blue) with the top 3 models in the overall DMS benchmark: Tranception (in orange) and MSA Transformer (in yellow), both of which are MSA-based, and ESM-1v (in light blue), which uses single sequence inputs. AIDO.Protein outperforms both MSA based models on most tasks, achieving performance close to ESM-1v.

Table 5: The impact of continuous training on AIDO.Protein-16B performance in the DMS zero-shot benchmark

Model	# Total Tokens	Score
AIDO.Protein-16B	1 trillion	0.401
AIDO.Protein-16B	1.2 trillion	0.405
AIDO.Protein-16B	1.3 trillion	**0.407**

Table 6: Comparison of AIDO.Protein with 1.3 trillion amino acids on selected DMS zeroshot tasks across various continuous training datasets

Model	Dataset	Score
AIDO.Protein-16B	Uniref50	0.364
AIDO.Protein-16B	Uniref90/50	0.389
AIDO.Protein-16B	Uniref90	**0.400**

A.3.2 Effects of continuous training dataset on model performance

We then discuss how the choice of continuous training datasets affects model performance. We continue training AIDO.Protein-16B, which has 1.2 trillion parameters, with an additional 100 billion tokens from three different datasets: UniRef90, UniRef50, and a sampled dataset combining UniRef90 and UniRef50. UniRef90 is a subset of UniMeta, while UniRef50 is a further clustered version of UniRef90. Inspired by ESM-2 [3], which proposes a sampling strategy to enhance data diversity and reduce redundancy by utilizing both UniRef90 and UniRef50, we adopt a similar approach to create the sampled dataset UniRef90/50. We randomly selected 50 zero-shot tasks from DMS zero-shot benchmark to compare the performance of these three continuous training models. The results are presented in Table 6. The model trained with Uniref90 achieves the best performance, while the model trained on both Uniref90 and Uniref50 outperforms the one solely trained on Uniref50, highlighting the benefits of utilizing Uniref90.

B Data and Code Availability

We developed the ModelGenerator package to reproduce, apply, and extend the results in this manuscript `https://github.com/genbio-ai/ModelGenerator`.

Pre-trained models and data splits are also available on Hugging Face at `https://huggingface.co/genbio-ai`.